A MODEL FOR PREDICTING THE PROBABILITY OF IMPINGEMENT OF JET FIRES

A.J.Carsley Shell Research Ltd., Thornton Research Centre, PO Box 1, Chester, CH1 3SH

The ability to predict jet fire impingement probabilities on objects can provide important input to scenario-based quantitative risk assessment (QRA) and can also be a useful aid in plant/platform design. The current Shell Research model for jet fires, while capable of making good predictions of flame lengths and radiative hazards from an estimated mean flame, has no facility for predicting the probability of impingement of flame on objects. Videos of existing large and small-scale experimental flame tests have been examined using image analysis techniques and data extracted on the spatial probability of occurrence of jet fires. The data have been used to formulate a general model for the spatial probability distribution of both vertically and horizontally released jet fires.

Key Words : fire, flame, jet, torch, impingement, image analysis

INTRODUCTION

The current Shell Research model for jet fires[1,2] , while capable of predicting flame lengths and radiative hazards from an estimated mean flame shape, has no facility for predicting the probability of flame impingement on an object and consequent heat transfer to that object. To fill this important gap requires a knowledge of flame variability. This knowledge exists in the form of spatial probability density data which were derived, using video image analysis techniques, from natural gas and propane horizontally released flame experiments[3]. Other unpublished data from lab-scale vertical natural gas jet fires have also been utilised. The data have been used to generate a general model for the spatial probability of flame occurrence for both vertically and horizontally released jet fires.

IMAGE ANALYSIS OF FLAMES

Videos of jet fire tests, both laboratory scale and large scale, have been used as input to a Kontron-based, full colour image analysis system running on a SUN workstation. In-house computer code has been written to drive the image analysis firmware and analyse the output. Typically, several hundred consecutive video frames are automatically frozen and analysed by the computer code. The system discriminates each flame from the background, i.e. the discriminated pixel image of an individual video frame will contain either 1 or 0 depending on whether there is flame at that point or not. A spatial probability distribution of the flame is constructed by summing the individually discriminated images.

A large number of releases have been analysed and consequently a small cross-section of these has been chosen to illustrate the probability model. These are:

Two, laboratory-scale, vertical releases of natural gas, one essentially laminar, test 9024, and the other a turbulent flame, test 9019.

A large-scale, horizontal, sonic release of natural gas, test 1002, flame type C as defined in Reference 3.

A large scale, horizontal, two-phase release of propane[3], test 3031.

THE FLAME SPATIAL PROBABILITY DISTRIBUTION MODEL

The mean flame

It is desirable that the mean flame should be defined within the overall probability of a flame occurrence model. Hence the approach used in generating the spatial probability model was to define a contour for the mean flame and then build the rest of the distribution around the mean flame. The 50% occurrence flame from the image analysis data was used to construct the model for the mean flame.

Vertical laboratory flames were chosen as a starting point for developing the flame spatial probability model. The measured spatial probability of occurrence of two, typical, vertically released methane diffusion flames (not pre-mixed) are shown in Figures 1 and 5 and the large-scale horizontal natural gas and propane releases are shown in Figures 9 and 13. On inspection of the 50% occurrence flame for the two vertical releases it can be seen that the two flame shapes are broadly similar but the low exit velocity flame is thinner at the base and thicker towards the tip of the flame. It was found that both mean flame shapes could be fitted by a simple two-parameter model,

$$w = a\xi^{p}\sqrt{-\ln(\xi)} \tag{1}$$

where ξ and w are dimensionless distances along the flame axis and normal to the flame axis respectively (the flame is assumed to be circular in cross-section normal to the flame axis and is scaled by its mean length with the mean flame tip at $\xi=1$, $w=0$), and the parameters a and p dictate the flame shape. From the above equation the maximum dimensionless flame full width can be shown to be given by,

$$w_m = ae^{-1/2}\sqrt{\frac{2}{p}}$$

$$\text{at} \qquad \xi = \xi_m = e^{-1/(2p)} \tag{2}$$

All the measured mean flame shapes have been found to give a remarkably good fit to this equation (using non-linear least squares techniques), see example Figures 2,6,10,14.

Theoretical support for equation (1) for the mean flame profile can be given if it is assumed that the visible flame is a measure of a concentration contour, e.g. the lower flammable limit, in a turbulent round jet[4,5]. Ignoring buoyancy forces and assuming the source diameter of the jet is small compared to the jet dimensions, for such a jet the centre-line concentration is expected to be inversely proportional to the distance x from the source,

$$C(x,0) = \frac{B}{x} \tag{3}$$

A Gaussian concentration profile normal to the jet axis, distance r from the axis, is assumed.

$$C(x,r) = C(x,0)\exp\left[\frac{-r^2}{2\sigma_r(x)^2}\right]$$

The usual assumption for a turbulent jet is that the width of this profile, which is expressed in terms of a standard deviation $\sigma_r(x)$, is proportional to x. However, equation (1) was found to be the best fit to the measured mean flame data and hence a more general assumption is now made that this width is a power law of x,

$$\sigma_r(x) = Ax^p$$

resulting in

$$C(x,r) = \frac{B}{x}\exp\left[\frac{-r^2}{2A^2x^{2p}}\right]$$

or, inverting

$$r = \sqrt{2}Ax^p\sqrt{-\ln\left(\frac{xC(x,r)}{B}\right)} \qquad (4)$$

The concentration is now set to equal to some value defining the limits of the mean flame profile, C_{50}. Then from (3) the length of the mean flame is $x_{50} = B/C_{50}$ and equations (4) and (1) are seen to be identical, when x and r are expressed in terms of the dimensionless flame co-ordinates ($x = \xi x_{50}$, $r = wx_{50}$), with $a = \sqrt{2}Ax_{50}^p$.

The probability of occurrence of flame along the centre-line

For horizontally released flames, which in practice bend upwards due to buoyancy effects, x is measured as the horizontal distance from the release point and r the half-width of the flame measured vertically. Similarly, for vertically released flames, x is measured as the vertical distance from the release point and r the half-width of the flame measured horizontally.

Centre-line probabilities of flame occurrence have been extracted from both the horizontal and vertical probability of occurrence data and plotted as a function of distance down the release axis, see example Figures 3,7,11,15. From inspection of these data it is observed that the ratio, R_t, of the distance from the source to the point on the flame centre-line where the 100% occurrence of the flame last occurs, x_{100}, to the length of the 50% occurrence flame, x_{50}, is virtually constant but has a different value depending on the flame release orientation.

For horizontally released flames x_{100} is predicted using,

$$x_{100} = (0.77 - 0.007v)x_{50} = R_t x_{50} \qquad (5)$$

where v is the wind speed in m/s. Note that at zero wind speed $x_{100} = 0.77x_{50}$ and at a 10m/s wind speed $x_{100} = 0.70x_{50}$, i.e. there is an increase in the width of the tail distribution with increasing wind speed. This correlation with wind speed is based on scant data from the natural gas horizontal releases, only two of the flames have wind speed in excess of 5 m/s, but it gives acceptable results for all observed horizontally releases flames. Note also that the correlation is independent of wind

direction. This is partly due to lack of data but intuitively it might also be expected that higher wind speeds will lead to more variable flames, whatever the wind direction.

For vertically released flames x_{100} is predicted using,

$$x_{100} = 0.68x_{50} = R_t x_{50} \tag{6}$$

Note that vertical flames are consistently observed to have a longer tail distribution than horizontally released flames. This correlation holds for both the laboratory vertical natural gas flames and limited data obtained from a PRV propane flame at Buxton[6]. Because of insufficient data (all the lab vertical flames tests were carried out in windless conditions) no attempt has been made to predict the effect of wind speed on the flame centre-line distribution for vertically released flames.

For all flames, the best fit for the form of the tail was found to resemble a normal distribution but with a power of 3 in the exponential term. This leads to a flatter top and steeper tail than the normal distribution,

$$P(x) = 100\exp\left\{-\left(\frac{x - x_{100}}{\sigma}\right)^3\right\} \quad \text{, for } x > x_{100}$$

$$P(x) = 100 \quad \text{, for } x < x_{100}$$

where $P(x)$ is the percent probability of occurrence of the flame along the flame centre-line. The function has a maximum value of 100% occurrence of flame at $x = x_{100}$ and is forced to take the value of $P(x)$=50 at $x = x_{50}$ by setting σ, the width parameter of the distribution to be,

$$\sigma = \frac{x_{50} - x_{100}}{\left[-\ln(0.5)\right]^{1/3}} = 1.13(x_{50} - x_{100})$$

Plots of the fitted distribution can also be seen in example Figures 3,7,11,15. Note that these distributions are fitted so that the end points of the fitted and measured mean flames are coincident. In practice, when predicting a flame distribution, there will be an error in the spatial location of the distribution caused by the accuracy of prediction of the mean flame end point by the flame model.

The general spatial probability of occurrence of flame

Having defined the 50% occurrence contour and the distribution of the tail of the flame, for other contours the shape is observed to be of the same form as the 50% mean flame with the width proportional to the square of the length. The following general expression is arrived at for the flame spatial probability distribution.

For the n% probability of flame occurrence contour, which has length x_n along the flame centre-line,

$$r = ax_n\left(\frac{x_n}{x_{50}}\right)^2\left(\frac{x}{x_n}\right)^p\sqrt{-\ln\left(\frac{x}{x_n}\right)} \tag{7}$$

where

$$x_n = \left[1.13(1 - R_t)\left(-\ln\left(\frac{P(x,r)}{100}\right)\right)^{1/3} + R_t\right]x_{50}$$

and $P(x,r)$ is the percent probability of flame occurrence at (x,r) in local flame co-ordinates.

Figures 4,8,12,16 show, for the selected flames, the fitted flame spatial probability of occurrence distributions using the model.

The flame shape parameters

The mean flame shape can be described by either the parameters a and p, or, alternatively, the parameters describing the dimensionless maximum flame width, w_m, and its location along the flame ξ_m, equations (1) and (2). The latter two parameters, which have more physical meaning and are orthogonal in terms of the flame co-ordinate axes, are the physical quantities measured from flame tests. Low exit velocity flames emanating from large-diameter, release holes are essentially gravity-dominated and give rise to lazy, laminar flames with large non-dimensional flame widths. Higher exit velocity flames from smaller diameter release holes are essentially momentum-dominated and have small non-dimensional flame widths. The flame width is also observed to have a strong dependence on wind speed. The flame mean length and width are supplied by the relevant flame model[1,2], thus providing the dimensionless parameter w_m. For horizontally released flames a correction is required,

$$w_m = (W_2 / \sin\theta_v) / (L_b \sin\theta_v) = \frac{W_2}{L_b \sin^2\theta_v}$$

where W_2 is the maximum flame width for the horizontally released flame and L_b is the straight line flame length from source to end of mean flame, and θ_v the angle the line joining the source and the end of the mean flame makes with the vertical, all predicted by the relevant flame model. Note that w_m is the ratio of the maximum flame width measured vertically to the horizontal projection of the flame length. This is necessary for consistency with the formulation of the flame probability model for horizontally release flames.

The dimensionless location of the maximum flame width, ξ_m, has been obtained from our flame data and plotted against Froude number (a measure of whether a flame is momentum or gravity-dominated, $Fr = u_j^2 / (gd_j)$ where u_j is the jet exit velocity and d_j the source diameter). For the vertical laboratory flames the location of ξ_m is observed to move towards the flame source at higher Froude numbers (more turbulent flames), see Figure 17. Larger scale vertical release data do not exist for this parameter, except for a measurement on an 11 m length propane pressure relief valve flame[6], which provides an additional supporting value of 0.645. The overall variation is rather small and hence an average value is used in the model. For vertically released flames,

$$\xi_m = 0.65$$

For the large scale horizontal releases of natural gas and propane, Figures 18 and 19, the data show the location of ξ_m is essentially independent of Froude number. For horizontally released natural gas flames,

$$\xi_m = 0.762$$

And for horizontally released two-phase propane and butane (assumed in the model to be the same as propane) flames,

$$\xi_m = 0.748$$

The flame centre-line trajectory for horizontally released flames

The dynamics of a horizontally released jet fire are dominated by the initial jet momentum, the air entrainment process and subsequent buoyancy of the hot ignited gases. Bosanquet et al[7]. have derived an expression for the path of a turbulent round jet of fluid injected into surroundings of different density at an arbitrary angle. The derivation assumes the well established hyperbolic mean velocity profile with distance down the jet[4] and conserves horizontal jet momentum. The expression has been approximated by Field et al. reference 5 Appendix F, to show that the path of such a jet closely follows a cubic equation,

$$y = x \tan \psi_0 + \frac{\beta}{3} x^3 \sec^2 \psi_0$$

where the jet is released at angle ψ_0 with the horizontal, and x and y are the horizontal and vertical axes respectively. Thus for a horizontally released jet,

$$y = \frac{\beta}{3} x^3 = cx^3$$

where β is a function of the jet source diameter, d_0, exit velocity , u_0, and initial densities of the jet , ρ_0, and surrounding medium, ρ_a

$$\beta = \frac{0.14 g(\rho_a - \rho_0)}{d_0 u_0^2 \rho_0 \cos \psi_0} \left(\frac{\rho_a}{\rho_0} \right)^{1/2} \tag{8}$$

The characteristics of an ignited jet will not be exactly the same as this non-ignited jet, e.g. the density will be a very strong function of flame temperature. However, this simple cubic equation has been fitted to the measured natural gas horizontal jet fire data and, in all cases, gives a good approximation to the flame centre-line. The measured flame data, in the form of spatial probability density functions, and the fitted centre-lines can be seen in Figures 9 and 13. The cubics are fitted through the release point and the end of the 50% occurrence mean flame. Note that equation (8) is not used in the impingement model. The constant c in the cubic equation is obtained using jet fire model predictions of the flame end-point (see next section).

THE PREDICTION OF PROBABILITY OF FLAME OCCURRENCE AT A POINT IN SPACE

Having defined a probability of occurrence of a flame in local flame co-ordinates it is required to find the probability of flame occurrence at a given point in 3-D space. This essentially means solving the non-linear equations (7) for P(x,r). However, the distances x and r must first be defined in the flame local co-ordinate system. The flame impingement model is set up to work in conjunction with the Shell Research jet fire model[1,2] which provides details of the release conditions and mean flame geometry, etc.. A global, positively oriented Cartesian co-ordinate system (X,Y,Z) is defined with the release point at the origin Figure 20 shows the global co-ordinate system used by the probability model together with typical vertically and horizontally released flames. The Shell Research model provides the following; the wind speed v, the net calorific value of the fuel C (used to determine the fuel type), the hole horizontal orientation with the X axis ϕ_h, the hole vertical orientation ϕ_v, the gas

exit velocity u_j , the flame length R_L , maximum width W_2 , lift-off b and horizontal and vertical orientations θ_h and θ_v.

Vertically released flames

As in the Shell Research jet fire models[1,2] the ignited release is assumed to have a non-combusting vertical lift-off distance and is then deflected by wind through an angle θ_v with the vertical (in the jet fire model the flame is represented by a tilted frustum of a cone). The flame centre-line is assumed to be straight. In the global co-ordinate system the end of the mean flame is at (see Figure 20),

$$X_2 = R_L \sin\theta_v \cos\theta_h$$
$$Y_2 = R_L \sin\theta_v \sin\theta_h$$
$$Z_2 = R_L \cos\theta_v + b$$

A virtual release point for the flame is created by extrapolating the flame centre line back by the lift-off distance b, this has global co-ordinates,

$$X_1 = -b \sin\theta_v \cos\theta_h$$
$$Y_1 = -b \sin\theta_v \sin\theta_h$$
$$Z_1 = b(1 - \cos\theta_v)$$

A check is made as to whether the flame release direction and the requested point in space (X_0, Y_0, Z_0) are in the same half-space, if not the point is behind the release point and the probability is set to zero, see Appendix for details.

The equation of the straight line running along the flame centre-line is generated and the nearest distance, r, of the point (X_0, Y_0, Z_0) from this line is calculated. Also calculated is the distance, x, along the flame axis from the source, of the normal from (X_0, Y_0, Z_0) to the flame centre-line. The Appendix contains the mathematical details of these three dimensional geometric calculations.

The distances in local flame co-ordinates along, x, and from, r, the flame axis of the requested point are now known. The parameter defining the tail of the probability distribution, R_t , is generated from equation (6) , section 3.2, and the flame shape parameters, as defined in section 3.4, are then used to find a and p. Equations (7) are then solved by a Newton-Raphson procedure to find the probability of flame occurrence $P(x,r)$.

Horizontally released flames

The centre-line of the flame is assumed to follow the path of a cubic having zero slope at the origin and passing through the end of the mean flame at (X_2, Y_2, Z_2). In the global co-ordinate system the end of the mean flame is located at (Figure 20).

$$X_2 = L_h \sin\theta_v \cos\theta_h$$
$$Y_2 = L_h \sin\theta_v \sin\theta_h$$
$$Z_2 = L_h \cos\theta_v$$

A check is made as to whether the flame release direction and the requested point in space (X_0, Y_0, Z_0) are in the same half-space, if not the point is behind the release point and the probability is set to zero, see Appendix for details.

The length of the mean flame in the local flame co-ordinate system is given by the projected length of the flame in the $Z=0$ plane,

$$x_{50} = L_h \sin\theta_v$$

The constant , c, defining the cubic for the flame centre-line is given by,

$$c = \frac{Z_2}{x_{50}^3}$$

A transformation is now required to the global axis system such that an observer at the point where the probability of flame occurrence is required sees the flame as being entirely horizontal. The transformation is achieved using the cubic equation for the flame centre-line, only the Z axis is transformed,

$$Z' = Z - c\left(\sqrt{X^2 + Y^2}\right)^3 \qquad (9)$$

In the transformed global co-ordinate system the flame is now seen as issuing horizontally from the origin at an angle θ_h with the X axis, with the mean flame tip at $(X_2, Y_2, 0)$ and the point where the probability of flame occurrence is required at $(X_0, Y_0, Z_0 - c\left(X_0^2 + Y_0^2\right)^{3/2})$. The distance of this point from the flame axis, r, and the distance, x, along the flame axis are found using the same method as for the vertical releases, see Appendix for details.

The parameter defining the tail of the probability distribution, R_t , is generated from equation (5) , section 3.2, and the flame shape parameters, as defined in section 3.4, are then used to find a and p. Equations (7) are then solved by a Newton-Raphson procedure to find the probability of flame occurrence $P(x,r)$.

CONCLUSIONS

1. A general model for the spatial probability distribution of a jet fire is developed. It is based on image analysis data of both large-and small-scale flame tests. It is shown that, for all the flames examined, the mean flame can be represented by a simple, two-parameter model. The spatial probability distribution for a flame has been built around the mean flame with the tail of the distribution along the flame centre-line resembling a normal type distribution with a power of 3 in the exponential term. Contours for other probabilities of flame occurrence have similar shape parameters to the mean flame.

2. Theory shows that the centre-line trajectory of horizontally released buoyant jet can be approximated by a simple cubic equation. Analysis of data from large-scale horizontally released, natural gas jet fires, measured using image analysis techniques, shows that the centre-line of such flames can also be adequately represented by a cubic equation, this behaviour is incorporated into the model.

REFERENCES

1. Chamberlain G.A., July 1987, Developments in design methods for predicting thermal radiation from flares, Chem Eng Res Des, Vol 65.

2. Johnson A.D., Brightwell H.M., Carsley A.J., August 1994, A model for predicting the thermal radiation hazards from large-scale horizontally released natural gas jet fires, Trans ICHEME, Vol 72, Part B.

3. Bennett J.F, Cowley L.T., Davenport J.N., Rowson J.J., 1991, Large scale natural gas and LPG jet fires final report to the CEC, CEC research programme: Major Technological Hazards, CEC contract EV4T.0016.UK, TNER.91.022 (Shell Research Ltd).

4. G.N.Abramovich, 1963, The theory of turbulent jets, MIT Press, Massachusetts Institute of Technology, Cambridge, Massachusetts.

5. M.A.Field et al, 1967, Combustion of pulverised coal, British Coal Utilisation research Association.

6. K.Moodie et al, June 1987, Total pool fire engulfment trials on a 5-tonne LPG tank; Part 1, Health and Safety Executive Research and Laboratory Services Division, IR/L/FR/87/27-1.

7. Bosanquet C.H, Horn G., and Thring M.W., 1961 Proc.R.Soc. Ser. A, 263,340-352.

8. Survey of Applicable Mathematics, Chapter 6, Solid Analytic Geometry, Frantisek Kejla.

1. NOMENCLATURE

A	Constant of proportionality defining variation of $\sigma_r(x)$ with x
a	Flame shape parameter, dimensionless
B	Constant of proportionality defining variation of flame centre-line concentration.
b	Flame lift-off, m
$C(x,r)$	Gas concentration of round jet at (x,r), units undefined.
c	Constant defining cubic equation for horizontally released flame centre-line
d_j	Flame source diameter, m
Fr	Froude number
g	Acceleration due to gravity, m/s-2
L_b	Straight line length of flame from source to end of mean flame, m
$P(x,r)$	Percent probability of flame occurrence at (x,r)
p	Flame shape parameter, dimensionless
R_L	Flame length from lift-off to end of mean flame, m
R_t	Ratio describing with of flame tail distribution, dimensionless
r	Distance from flame axis (centre-line) in local flame co-ordinates, m
u_j	Expanded source gas exit velocity
v	Wind speed, m/s
W_2	Maximum flame width, m
w	Mean flame width, dimensionless
w_m	Maximum width of the mean flame, dimensionless
x	Distance along flame axis (centre-line) from source in local flame co-ordinates, m
X,Y,Z	Global Cartesian co-ordinate system, m
Z'	Transformed global Z co-ordinate used for horizontal flames, m
Ψ_0	Release angle of jet to horizontal
β	Parameter used to describe cubic equation for flame centre-line
θ_h	Angle of flame to global X axis, degrees
θ_v	Angle of flame to vertical, degrees
ϕ_h	Angle of release direction to global X axis, degrees
ϕ_v	Angle of release direction to vertical, degrees
ρ	Density of gas
σ	Width parameter of probability distribution for tail of flame, m
$\sigma_r(x)$	Width parameter of concentration distribution normal to turbulent jet axis.
ξ	Distance along axis of mean flame, dimensionless
ξ_m	Distance to maximum flame width along axis of mean flame, dimensionless

Additional subscripts.

0	Global location of point where probability of flame occurrence required
1	Global location of flame source, or virtual source for vertical releases
2	Global location of end of mean flame
50	Mean flame (50% occurrence contour)
100	100% occurrence contour
n	n% contour

APPENDIX

Theorems given in Reference 8 have been used to provide support for the following three dimensional co-ordinate geometry.

For both vertical and horizontal releases the problem has been reduced to the case where the flame has source, or virtual source in the case of vertical releases, at (X_1, Y_1, Z_1) with its axis (centre-line) being straight and passing through the end of the mean flame at (X_2, Y_2, Z_2). The probability of flame occurrence is required at point (X_0, Y_0, Z_0). Note that the same global co-ordinate system as defined in section 4 is used here, with the exception that, for horizontal releases the Z axis has been transformed using the transformation given in section 4.2, equation (9).

Because of the method of calculation, which returns scalar distances, a check is required that the point (X_0, Y_0, Z_0) is in the same half-space as the flame. The equation of the plane passing through (X_1, Y_1, Z_1) and normal to the release direction is,

$$\cos\theta_h(X - X_1) + \sin\theta_h(Y - Y_1) + \cos\theta_v(Z - Z_1) = 0$$

The above equation is evaluated at (X_2, Y_2, Z_2) and (X_0, Y_0, Z_0), if the two results are of opposite sign then (X_0, Y_0, Z_0) is not in the same half-space as the flame (this is an established theorem). No further calculation is required and the probability of flame occurrence is returned as zero.

The equation if the straight line running along the flame axis, passing through (X_1, Y_1, Z_1) and (X_2, Y_2, Z_2) is ,

$$\frac{X - X_1}{X_2 - X_1} = \frac{Y - Y_1}{Y_2 - Y_1} = \frac{Z - Z_1}{Z_2 - Z_1}$$

The distance of the point (X_0, Y_0, Z_0) from this line is required, this is the distance r from the flame axis in local flame co-ordinates. It is given by (established theorem),

$$r = \frac{|\mathbf{m} \otimes \mathbf{n}|}{|\mathbf{n}|}$$

where $\mathbf{m} = (X_0 - X_1, Y_0 - Y_1, Z_0 - Z_1)$ and $\mathbf{n} = (X_2 - X_1, Y_2 - Y_1, Z_2 - Z_1)$

$$\mathbf{m} \otimes \mathbf{n} = (Y_0 Z_2 - Y_2 Z_0, X_0 Z_2 - X_2 Z_0, X_0 Y_2 - X_2 Y_0)$$

$$= (XX, YY, ZZ)$$

$$|\mathbf{m} \otimes \mathbf{n}| = \sqrt{XX^2 + YY^2 + ZZ^2}$$

and,

$$|\mathbf{n}| = \sqrt{(X_2 - X_1)^2 + (Y_2 - Y_1)^2 + (Z_2 - Z_1)^2}$$

The distance, x, along the flame axis from the flame source, is then given by Pythagoras,

$$x = \sqrt{(X_0 - X_1)^2 + (Y_0 - Y_1)^2 + (Z_0 - Z_1)^2 - r^2}$$

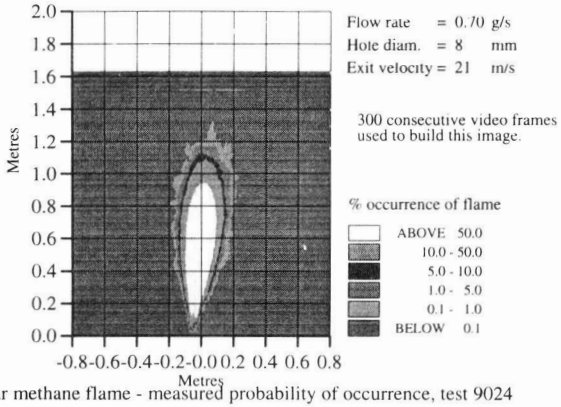

Fig.1 Laminar methane flame - measured probability of occurrence, test 9024

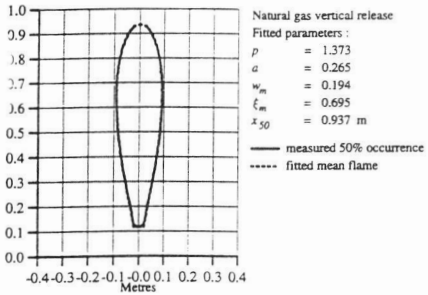

Fig.2 Measured and fitted 50% occurrence flame, test 9024

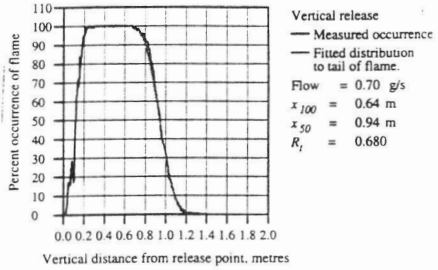

Fig. 3 Flame p.d.f. centre-line profile, test 9024, natural gas

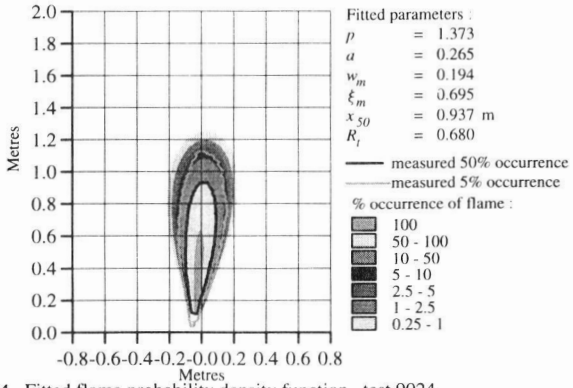

Fig.4 Fitted flame probability density function , test 9024

APPENDIX

Theorems given in Reference 8 have been used to provide support for the following three dimensional co-ordinate geometry.

For both vertical and horizontal releases the problem has been reduced to the case where the flame has source, or virtual source in the case of vertical releases, at (X_1, Y_1, Z_1) with its axis (centre-line) being straight and passing through the end of the mean flame at (X_2, Y_2, Z_2). The probability of flame occurrence is required at point (X_0, Y_0, Z_0). Note that the same global co-ordinate system as defined in section 4 is used here, with the exception that, for horizontal releases the Z axis has been transformed using the transformation given in section 4.2, equation (9).

Because of the method of calculation, which returns scalar distances, a check is required that the point (X_0, Y_0, Z_0) is in the same half-space as the flame. The equation of the plane passing through (X_1, Y_1, Z_1) and normal to the release direction is,

$$\cos\theta_h(X - X_1) + \sin\theta_h(Y - Y_1) + \cos\theta_v(Z - Z_1) = 0$$

The above equation is evaluated at (X_2, Y_2, Z_2) and (X_0, Y_0, Z_0), if the two results are of opposite sign then (X_0, Y_0, Z_0) is not in the same half-space as the flame (this is an established theorem). No further calculation is required and the probability of flame occurrence is returned as zero.

The equation if the straight line running along the flame axis, passing through (X_1, Y_1, Z_1) and (X_2, Y_2, Z_2) is ,

$$\frac{X - X_1}{X_2 - X_1} = \frac{Y - Y_1}{Y_2 - Y_1} = \frac{Z - Z_1}{Z_2 - Z_1}$$

The distance of the point (X_0, Y_0, Z_0) from this line is required, this is the distance r from the flame axis in local flame co-ordinates. It is given by (established theorem),

$$r = \frac{|\mathbf{m} \otimes \mathbf{n}|}{|\mathbf{n}|}$$

where $\mathbf{m} = (X_0 - X_1, Y_0 - Y_1, Z_0 - Z_1)$ and $\mathbf{n} = (X_2 - X_1, Y_2 - Y_1, Z_2 - Z_1)$

$$\mathbf{m} \otimes \mathbf{n} = (Y_0 Z_2 - Y_2 Z_0, X_0 Z_2 - X_2 Z_0, X_0 Y_2 - X_2 Y_0)$$

$$= (XX, YY, ZZ)$$

$$|\mathbf{m} \otimes \mathbf{n}| = \sqrt{XX^2 + YY^2 + ZZ^2}$$

and,

$$|\mathbf{n}| = \sqrt{(X_2 - X_1)^2 + (Y_2 - Y_1)^2 + (Z_2 - Z_1)^2}$$

The distance, x, along the flame axis from the flame source, is then given by Pythagoras,

$$x = \sqrt{(X_0 - X_1)^2 + (Y_0 - Y_1)^2 + (Z_0 - Z_1)^2 - r^2}$$

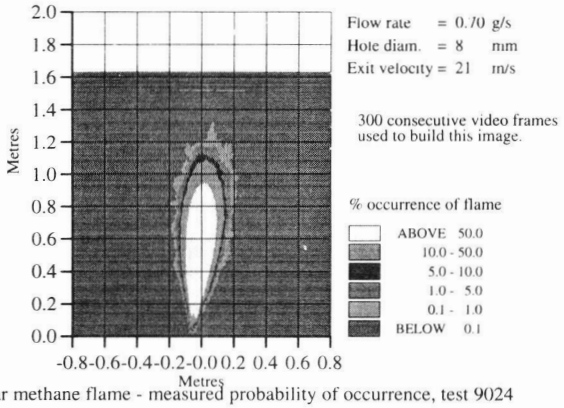

Fig.1 Laminar methane flame - measured probability of occurrence, test 9024

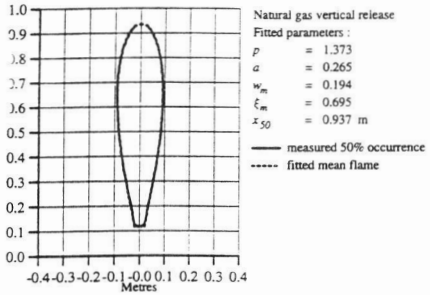

Fig.2 Measured and fitted 50% occurrence flame, test 9024

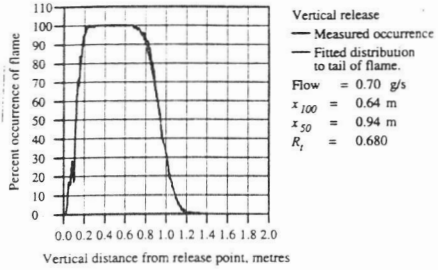

Fig. 3 Flame p.d.f. centre-line profile, test 9024, natural gas

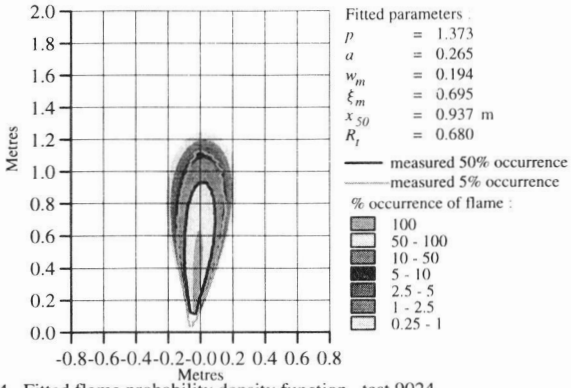

Fig.4 Fitted flame probability density function , test 9024

APPENDIX

Theorems given in Reference 8 have been used to provide support for the following three dimensional co-ordinate geometry.

For both vertical and horizontal releases the problem has been reduced to the case where the flame has source, or virtual source in the case of vertical releases, at (X_1, Y_1, Z_1) with its axis (centre-line) being straight and passing through the end of the mean flame at (X_2, Y_2, Z_2). The probability of flame occurrence is required at point (X_0, Y_0, Z_0). Note that the same global co-ordinate system as defined in section 4 is used here, with the exception that, for horizontal releases the Z axis has been transformed using the transformation given in section 4.2, equation (9).

Because of the method of calculation, which returns scalar distances, a check is required that the point (X_0, Y_0, Z_0) is in the same half-space as the flame. The equation of the plane passing through (X_1, Y_1, Z_1) and normal to the release direction is,

$$\cos\theta_h(X - X_1) + \sin\theta_h(Y - Y_1) + \cos\theta_v(Z - Z_1) = 0$$

The above equation is evaluated at (X_2, Y_2, Z_2) and (X_0, Y_0, Z_0), if the two results are of opposite sign then (X_0, Y_0, Z_0) is not in the same half-space as the flame (this is an established theorem). No further calculation is required and the probability of flame occurrence is returned as zero.

The equation if the straight line running along the flame axis, passing through (X_1, Y_1, Z_1) and (X_2, Y_2, Z_2) is ,

$$\frac{X - X_1}{X_2 - X_1} = \frac{Y - Y_1}{Y_2 - Y_1} = \frac{Z - Z_1}{Z_2 - Z_1}$$

The distance of the point (X_0, Y_0, Z_0) from this line is required, this is the distance r from the flame axis in local flame co-ordinates. It is given by (established theorem),

$$r = \frac{|\mathbf{m} \otimes \mathbf{n}|}{|\mathbf{n}|}$$

where $\mathbf{m} = (X_0 - X_1, Y_0 - Y_1, Z_0 - Z_1)$ and $\mathbf{n} = (X_2 - X_1, Y_2 - Y_1, Z_2 - Z_1)$

$$\mathbf{m} \otimes \mathbf{n} = (Y_0 Z_2 - Y_2 Z_0, X_0 Z_2 - X_2 Z_0, X_0 Y_2 - X_2 Y_0)$$

$$= (XX, YY, ZZ)$$

$$|\mathbf{m} \otimes \mathbf{n}| = \sqrt{XX^2 + YY^2 + ZZ^2}$$

and,

$$|\mathbf{n}| = \sqrt{(X_2 - X_1)^2 + (Y_2 - Y_1)^2 + (Z_2 - Z_1)^2}$$

The distance, x, along the flame axis from the flame source, is then given by Pythagoras,

$$x = \sqrt{(X_0 - X_1)^2 + (Y_0 - Y_1)^2 + (Z_0 - Z_1)^2 - r^2}$$

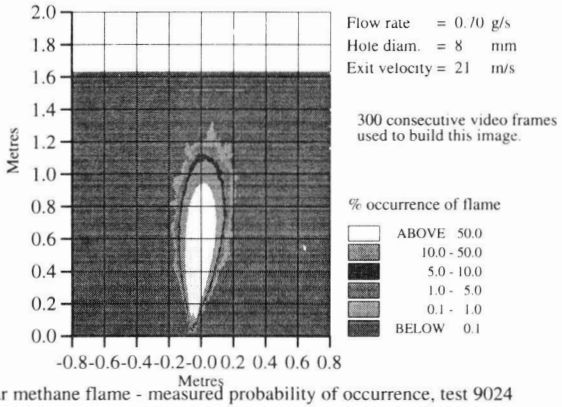

Fig.1 Laminar methane flame - measured probability of occurrence, test 9024

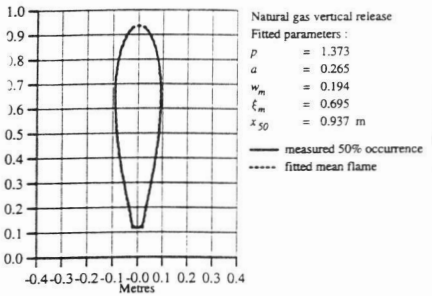

Fig.2 Measured and fitted 50% occurrence flame, test 9024

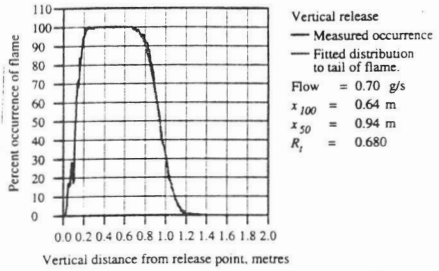

Fig. 3 Flame p.d.f. centre-line profile, test 9024, natural gas

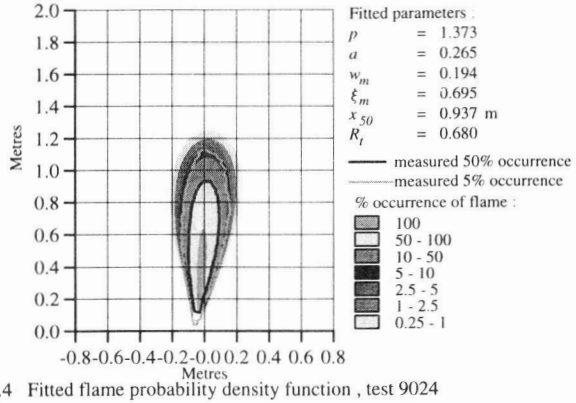

Fig.4 Fitted flame probability density function , test 9024

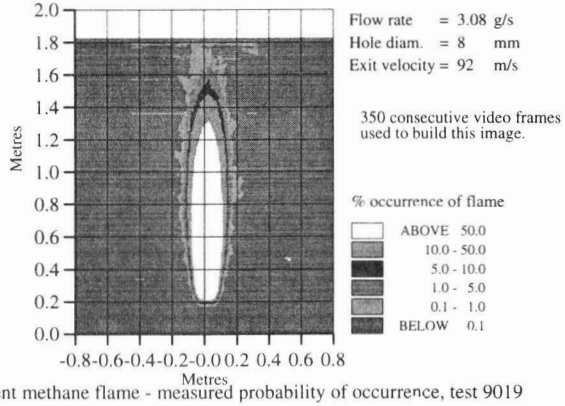

Fig.5 Turbulent methane flame - measured probability of occurrence, test 9019

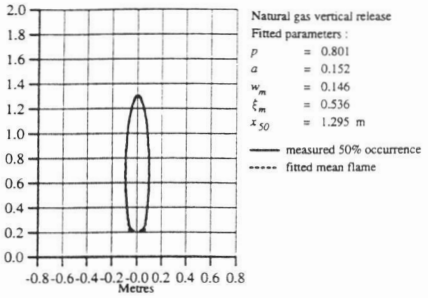

Fig.6 Measured and fitted 50% occurrence flame, test 9019

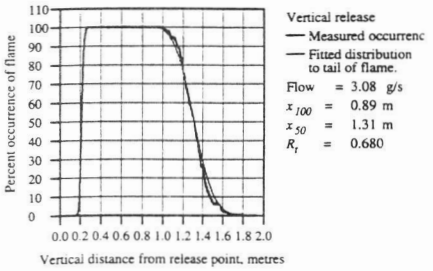

Fig. 7 Flame p.d.f. centre-line profile, test 9019, natural gas

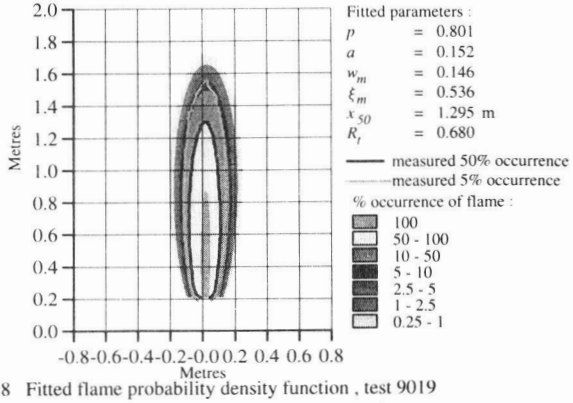

Fig.8 Fitted flame probability density function , test 9019

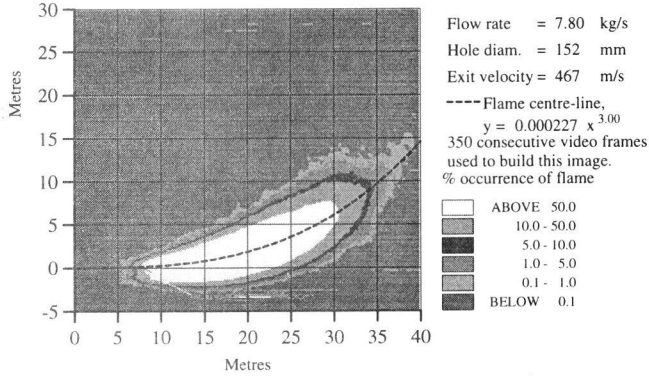

Fig.9 Measured probability of occurrence, test 1002, natural gas

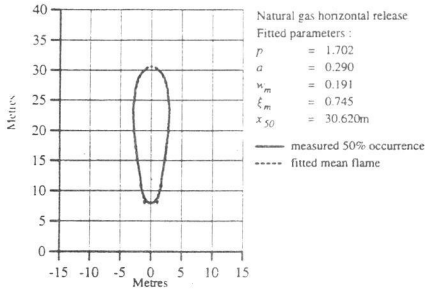

Fig.10 Measured and fitted 50% occurrence flame, test 1002

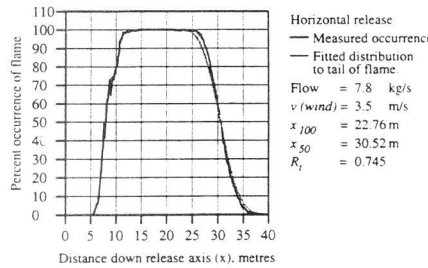

Fig.11 Flame p.d.f. centre-line profile, test 1002, natural gas

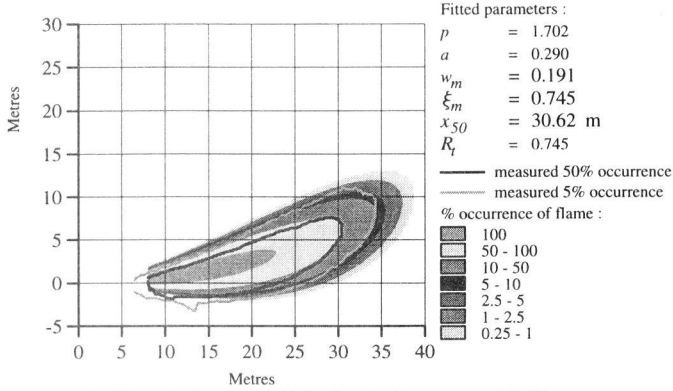

Fig.12 Fitted flame probability density function , test 1002

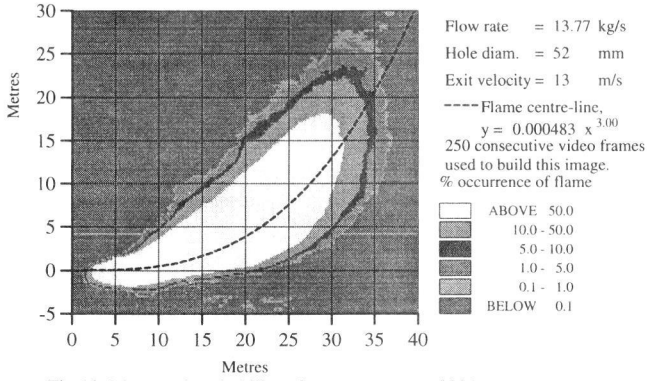

Fig.13 Measured probability of occurrence, test 3031, propane

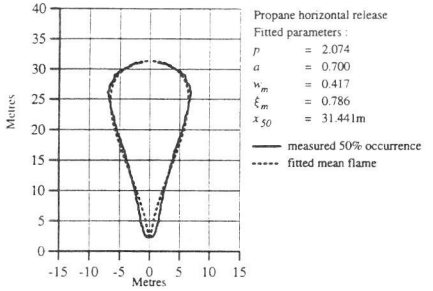

Fig.14 Measured and fitted 50% occurrence flame, test 3031

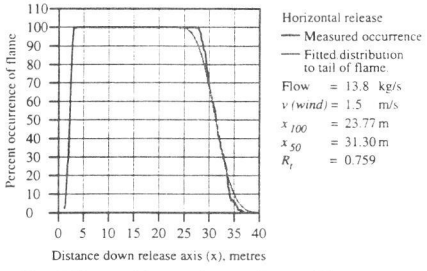

Fig.15 Flame p.d.f. centre-line profile, test 3031, propane

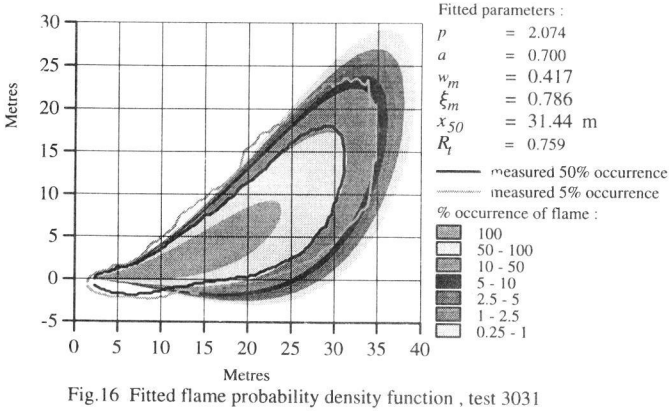

Fig.16 Fitted flame probability density function , test 3031

Fig.17 Position of maximum flame width vs log(Fr)

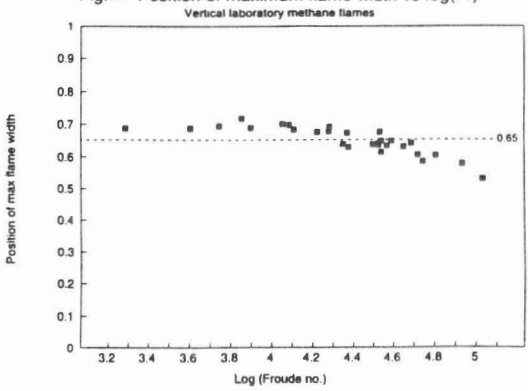

Fig.18 Position of maximum flame width vs log(Fr)

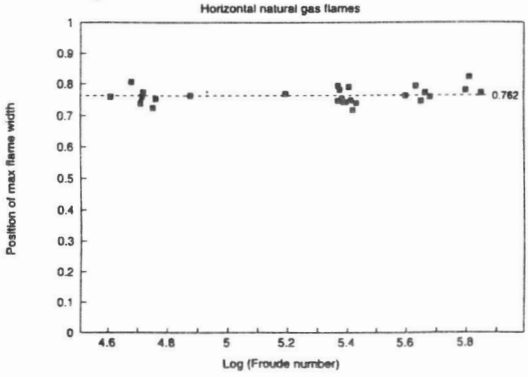

Fig.19 Position of maximum flame width vs log(Fr)

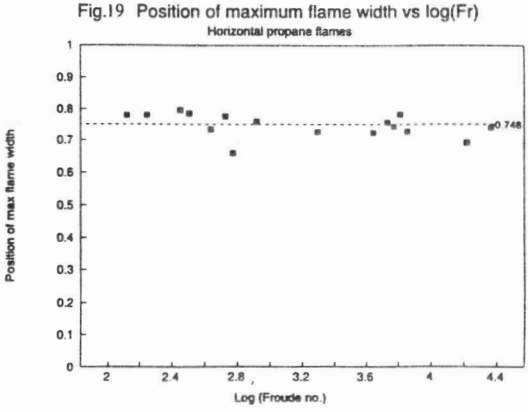

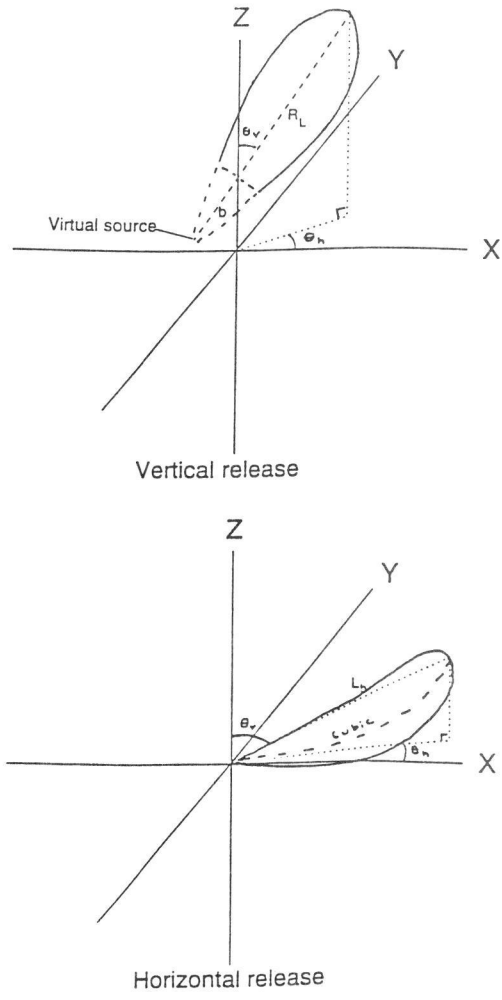

Fig. 20 Global coordinate system